Surface phase behavior in binary polymer mixtures. I. Miscibility, phase coexistence, and interactions in polyolefin blends

Frank Scheffold, Erika Eiser, Andrzej Budkowski, Ullrich Steiner, and Jacob Klein
Department of Materials and Interfaces, Weizmann Institute of Science, Rehovot 76100, Israel

Lewis J. Fetters
Exxon Research and Engineering Company, Annadale, New Jersey 08801

(Received 18 December 1995; accepted 29 February 1996)

We have used composition depth profiling of polymer bilayers, based on nuclear reaction analysis, to determine miscibility, phase coexistence, and critical temperatures in mixtures of random olefinic copolymers of mean composition E_{1-x}/EE_x; here E is the ethylene group $-(C_4H_8)-$, EE is the ethylethylene group $-[C_2H_3(C_2H_5)]-$, and one of the copolymers is partially deuterated. The components in each binary mixture have different values x_1, x_2 of the EE fraction. Using a simple Flory–Huggins mixing model, our results enable us to extract an interaction parameter of the form $\chi(x_1, x_2, T) = A(x_1, x_2)/T$, where for given x_1, x_2, A is a constant. Calculated binodals using this form fit our measured coexistence curves well, while allowing χ a weak composition dependence improves the fit further. Within the range of our parameters, our results suggest that in such binary polyolefin mixtures the interaction parameter increases roughly linearly with the extent of chemical mismatch expressed as the difference in degree of ethyl branching between the two components.
 [S0021-9606(96)51321-8]

I. INTRODUCTION

In earlier work we investigated surface segregation and wetting behavior in mixtures of random olefinic copolymers.[1–4] These copolymers, of structure $(E_{1-x}EE_x)_N$, where E and EE ethylene and ethyl ethylene groups, respectively, are chains whose mean microstructure varies continuously with x from polyethylene ($x=0$) to poly(ethyl ethylene), $x=1$. Since the two monomer species are isomers of (C_4H_8), itself a nonpolar group, the variation in properties as x changes is relatively gentle. Several physical properties of these E/EE copolymers have been comprehensively studied as a function of the change in mean microstructure. These include their bulk viscoelastic properties,[5,6] their self-diffusion coefficients,[7] and the unperturbed chain dimensions and Kuhn step lengths of the molecules over a wide range of x values.[8–11] Such polymers, quite apart from the technological importance of polyolefins in materials applications, provide very useful model systems for investigating bulk and interfacial properties of binary mixtures: by studying mixtures of two E/EE polymers, with different fractions x_1, x_2 of the ethyl-branched components, the extent of both bulk and surface interactions may, in principle, be tuned through judicious choice of the two x values. In addition to their surface segregation behavior, the properties of such x_1/x_2 mixtures have been investigated in several studies. These include their scattering properties,[10–13] their coexistence characteristics,[14,15] and the interfacial widths between coexisting phases.[15]

Our earlier results, using a blend of these E/EE copolymers as a model binary system, demonstrated that complete wetting could occur in polymer mixtures.[1,2] The aim of the present work is to understand the factors—in particular the microstructural composition—that preferentially drive the chains in such polyolefinic blends to surfaces, and to gain insight into the conditions which determine whether wetting from such mixtures will be complete[1] or partial.[3,4] To this end we examine systematically the properties of E/EE binary mixtures using several random copolymers covering the range $x=0.38$–0.97. Since any quantitative discussion of the interfacial properties in such mixtures must involve knowledge also of their bulk thermodynamics, the present study has a twofold focus. In this paper (Paper I) we use nuclear reaction analysis (NRA) to investigate the miscibility, coexistence characteristics, critical temperatures, and segmental interaction parameters of a series of 12 different blends of these copolymers. In the second paper (II) we carry out a comprehensive investigation of the interfacial properties of these same blends at different surfaces. In the third paper (III) we examine in detail the surface segregation behavior from such blends at different temperatures, and consider the expected wetting and wetting-transition characteristics using the bulk thermodynamic information derived here for the identical mixtures.

II. EXPERIMENTAL SECTION

A. Materials

The materials used for this study are 14 different model polyolefins, seven fully hydrogenous and seven partially deuterated. These polymers consist of branched ethyl–ethylene units (designated EE) and linear di-ethylene units (referred to simply as ethylene or E), randomly distributed along the chain as shown

 0021-9606/96/104(21)/8786/9/$10.00

TABLE I. Molecular parameters of model polyolefins. Molecular characteristics of the $P(E\text{-}EE)$ model polyolefins. N is the degree of polymerization, n_b the number of branches per 100 carbon backbone units, and f_D denotes the fractional deuteration of the deuterated sample.

Sample	% EE	n_b	N	f_D
$d38/h38$	38	11.7	1830	0.37
$d52/h52$	52	17.6	1510	0.34
$d66/h66$	66	24.6	2030	0.40
$d75/h75$	75	30.0	1625	0.40
$d86/h86$	86	37.7	1520	0.40
$d94/h94$	94	44.3	707	0.30
$d97A/h97A$	97	47.1	1600	0.35

$$[\{CH_2-CH\}_x-\{CH_2-CH_2-CH_2-CH_2\}_{1-x}]$$

(side group on CH: $|$ CH_2 $|$ CH_3)

↑ ethylethylene $(EE)_x$ ↑ di-ethylene $(E)_{1-x}$.

Chains are designated hx or dx, where x specifies the EE content of a chain, i.e., the fraction of branched monomer units (for clarity, x in these designations is in percent), and the prefix letter denotes whether the chains are hydrogenous or partially deuterated; thus $d66$ is a partially deuterated chain with $x=0.66$ (or 66%). The materials were obtained by anionic polymerization of the precursor unsaturated PBD chains, as described in detail earlier,[10] and are nearly monodisperse ($M_w/M_n<1.08$ in all cases). The precursor samples were divided and each half was subjected to hydrogenation or deuteration to the saturated state, so that the ethyl-content x and degree of polymerization are identical for the hydrogenated sample and the deuterated counterpart.

It is sometimes useful to consider the number of ethyl branches per 100 carbon backbone units n_b rather than x. The relation between them is

$$n_b=\frac{x}{4-2x/100}. \tag{1}$$

The molecular characteristics of the polymers, including weight averaged degrees of polymerization and the deuteration fraction are given in Table I. The glass transition temperatures of the bulk copolymers varied from $-22\,°C$ for $x=97\%$ to $-62\,°C$ for $x=38\%$.

The coexistence characteristics of these materials were studied as previously described,[15,16] by creating a bilayer of the pure copolymers and allowing the two layers to interdiffuse to equilibrium. At temperatures below the critical temperature T_c interdiffusion occurs until the compositions on either side of the interface reach their coexistence values. These are then determined using NRA to provide the composition–depth profile of the bilayer. Use of NRA necessitates deuterium labeling of one of the components, so the bilayers (and the final coexisting phases) in all cases consist of a partially deuterated and a fully hydrogenated component.

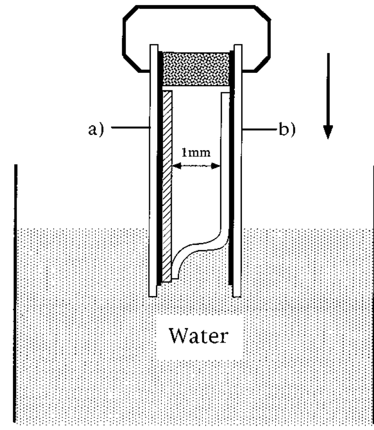

FIG. 1. A schematic of the jig used to create a bilayer of two E/EE films. One of the films is spin cast onto a mica sheet and floated as indicated onto a second film spin cast on a silicon wafer, to create the bilayer. a and b are glass slides clamped together 1 mm apart, holding the silicon wafer and the film-bearing mica sheet as shown. The jig is slowly lowered into the water bath, and the water meniscus rising up the hydrophilic mica surface pushes one film, with little distortion, onto the other as indicated.

Polished silicon wafers (obtained from Aurel GmbH, Germany) were used as the supporting substrate for the bilayers. The silicon wafers were either degreased in toluene solution (which leaves a thin SiO_2 layer on each wafer), or covered with an evaporated high-purity smooth gold layer (thickness ~20 nm).

Thin films (mean thickness in the range 450 ± 50 nm, uniform to within a few nm) of the pure components were prepared by spin coating the wafers with solutions of the polymers in toluene. To create the bilayers a second layer was spin cast on mica and then transferred on top of the first one. Since at room temperature, where the bilayers are created, the polymers are far above their glass transition points, floating them on water results in films which rapidly contract (and thicken) due to their hydrophobicity. To avoid this and ensure that the transferred films retain their as-cast integrity, a transfer jig, illustrated in Fig. 1, was used.

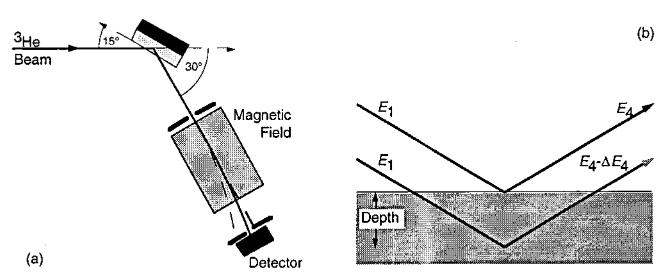

FIG. 2. The geometry of the NRA setup used to profile the composition-depth characteristics of the deuterated polymer chains in these experiments. (a) The magnetic field only allows the required particles to-pass through. (b) A magnified scale of the sample. The energy loss ΔE_4 of the 4He particles reveals the depth at which the reaction occurred.

TABLE II. Critical temperatures of polyolefin blends. Miscibilities and critical temperatures for all available blends. The bold numbers are values of T_c (in °C) based on the binodals in Figs. 4–9; those in normal type are evaluated from determination of the ratios of the coexisting compositions (see Fig. 10). The blends marked with X are not miscible for temperatures $T \leqslant 250$ °C (see text), while those marked with dots (···) had an even larger chemical mismatch and were not investigated (see text).

	*d*38	*d*52	*d*66	*d*75	*d*86	*d*94	*d*97
*h*38	*	77±7	*X*	···	···	···	···
*h*52	50±10	*	**204**	*X*	···	···	···
*h*66	*X*	**88**	*	**101**	*X*	···	···
*h*75	···	*X*	33±10	*	**181**	*X*	···
*h*86	···	···	*X*	**97**	*	**50**	223±5
*h*94	···	···	···	*X*	<30	*	<30
*h*97	···	···	···	···	75±10	<30	*

The bilayer samples (wafer size $\sim 1 \times 1.5$ cm^2) were annealed for times which varied with the annealing temperature, but were in all cases sufficient to ensure that the interdiffusing layers had reached their final equilibrium compositions. This was indicated by control measurements of the variation of the coexisting phase compositions with time,[16] and also by direct measurements of the diffusion coefficients of the component copolymers.[7] For temperatures above 70 °C, due to the high mobility of the model polyolefins used in this study, annealing times of less than a day or two were sufficient to reach equilibrium. In this temperature range the samples were either annealed in a high stability (±1 °C) vacuum oven (10^{-3} bar) or, at the highest temperatures, they were sealed in glass ampoules under vacuum ($<10^{-5}$ Torr) in order to prevent degradation. For temperatures below 70 °C the samples were sealed and annealed at normal pressure in a temperature stabilized liquid bath (±0.2 °C) or in a temperature stabilized room (±0.5 °C) for up to two months. After annealing the samples were quenched very rapidly to a temperature (<−80 °C) below the glass transition temperature and stored at this temperature until required for the experiments.

NRA was used to monitor the composition profile of the deuterated species in the polymer bilayers following annealing. NRA is described in detail elsewhere[17–19] and we restrict ourselves here to the basic principles and the configuration, illustrated in Fig. 2, used to determine the coexisting compositions. A monoenergetic ^{3}He beam of energy E_1 impinges on and penetrates into the polymer sample at a forward angle of 15°. At different depths x inside the sample an exothermic nuclear reaction takes place (with a certain energy-dependent cross section) between the incoming ^{3}He and deuterium atoms in the sample

$$^3\mathrm{He} + {}^2\mathrm{H} \rightarrow {}^4\mathrm{He} + {}^1\mathrm{H} + Q, \quad Q = 18.4 \ \mathrm{MeV}. \tag{2}$$

The outgoing charged ^{4}He (α) particles are detected at a forward angle after emerging the sample. The arrangement is shown schematically in Fig. 2. The energy ($E_4 - \Delta E_4$) of the outgoing α particles is determined by the depth x within the sample at which the reaction took place. This is because the incoming ^{3}He and the outgoing ^{4}He both lose energy in traversing the sample: based on the kinematics of the nuclear reaction and the energy loss within the sample, the depth in which the reaction took place can be calculated. Normalizing with respect to the reaction cross section provides a relative composition–depth profile of the deuterium atoms, and thus of the polymer chains which they label.

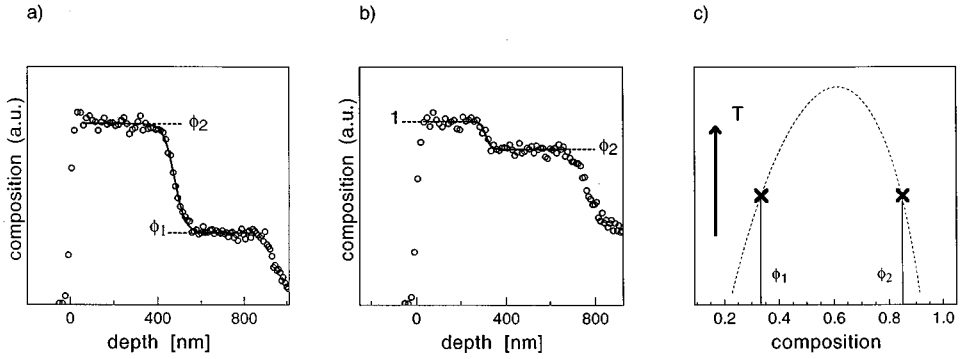

FIG. 3. (a) A typical NRA depth vs concentration profile of the annealed bilayer. The data points correspond to the local concentration of deuterium, i.e., of the segments of the deuterated component. This allows the evaluation of the ratio of the coexisting concentrations ϕ_1/ϕ_2, though not their absolute values. (b) In order to normalize the spectrum, an additional layer of pure deuterated material has to be floated onto the annealed bilayer. Putting together the information obtained from the first and the second NRA spectrum yields absolute values of ϕ_1 and ϕ_2. (c) If this procedure is carried out for different temperatures a phase diagram of the polymer blend can be determined (dashed line). The example was taken from the determination of the phase diagram of the *d*75/*h*66 blend with an annealing temperature of $T = 65$ °C.

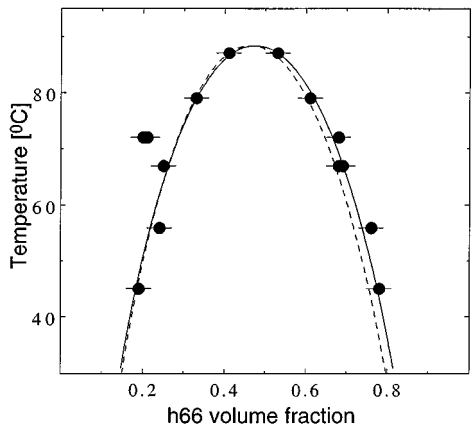

FIG. 4. Experimentally determined phase coexistence diagram (binodal) of the blend $d52/h66$, determined as described in text and Fig. 3. From the binodal, the critical temperature for this blend is $T_c=88\pm4$ °C. The broken curve is the binodal calculated from the FH model with $\chi(T)=A/T$. The solid line represents the best fit to the experimental data, calculated from the FH model with a ϕ-dependent interaction parameter $\chi(T,\phi)=(A'T+B)(1+v\phi)$. The parameters A, A', B, and v are given in Table III.

III. RESULTS

Miscibility and coexistence characteristics were investigated for all possible binary blends dx_i/hx_j where i and j $(i\neq j)$ refer to different samples in Table I. The matrix of the different binary combinations is shown in Table II. Uniform layers of the two polyolefins were mounted on the silicon or gold-covered silicon wafers to form a bilayer system. Heating the bilayer at a temperature $T<T_c$ leads to molecular transport across the interface between the initially pure layers, driving their compositions towards their coexisting values ϕ_1 and ϕ_2. For temperatures above T_c the two layers will fully interdiffuse resulting in a uniform layer, hence setting an upper limit for T_c. Annealing was carried out until steady state was achieved; the composition profiles were then determined, and constitute the primary experimental output of this study. Figure 3(a) shows a typical concentration-depth profile obtained by NRA. We note that in all cases the thickness of the bilayer samples (at ~800–1000 nm) greatly exceeds both the radii of gyration of the chains (~10 nm) and the interfacial widths or the bulk correlation lengths (generally <30 nm) within the mixtures over the range of experimental conditions studied, ensuring that finite size effects on the coexistence characteristics[20,21] are negligible.

NRA provides a relative measure of the composition profile of the deuterated chains across the sample. In order to determine the absolute value of the coexisting compositions, the bilayer [after the initial profiling to determine the ratio ϕ_1/ϕ_2 of the coexisting compositions, Fig. 3(a)] is covered with an additional layer of known concentration and measured again. This then yields the absolute value of both coexisting compositions, which provide two points on the phase coexistence diagram at the annealing temperature used. The procedure is illustrated in Figs. 3(b) and 3(c). Using this method the detailed phase coexistence diagrams were determined for six of the polyolefin blends, and are shown in Figs. 4–9. The dashed horizontal lines in Figs. 4–9 indicate the temperatures at which complete interdiffusion was observed. The broken and solid curves in Figs. 4–9 are

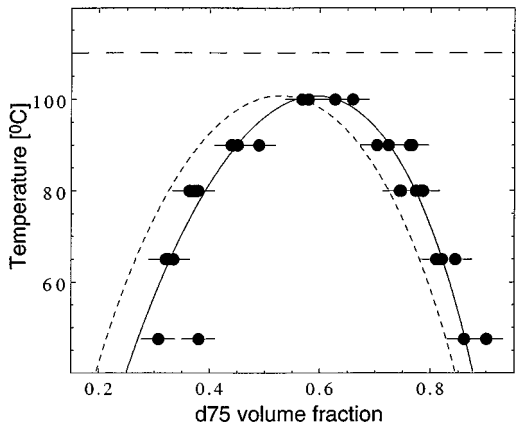

FIG. 6. Binodal for the blend $d75/h66$. From the binodal, the critical temperature for this blend is $T_c=101\pm4$ °C. Curves and broken horizontal line as described in Figs. 4 and 5.

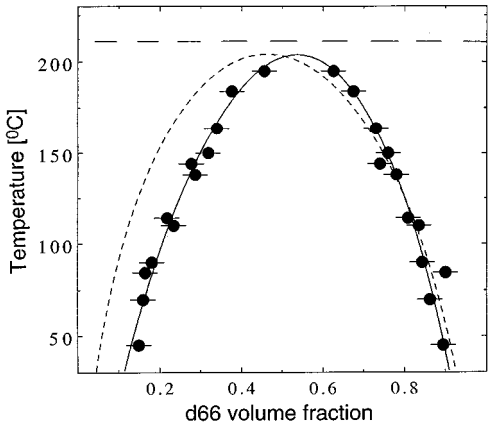

FIG. 5. Binodal for the blend $d66/h52$. The broken horizontal line indicates an annealing temperature T at which full interdiffusion was observed, i.e., $T>T_c$. From the binodal, the critical temperature for this blend is $T_c=204\pm4$ °C. Curves as described in Fig. 4.

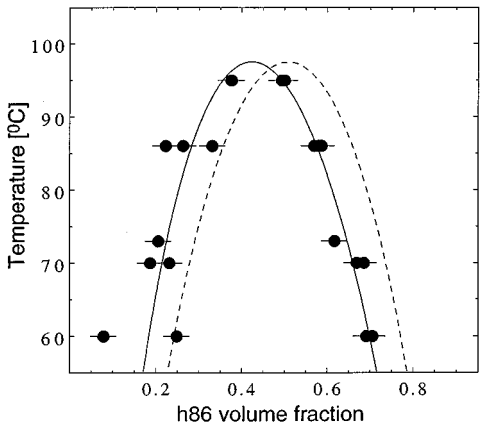

FIG. 7. Binodal for the blend $d75/h86$. From the binodal, the critical temperature for this blend is $T_c=97\pm4$ °C. Curves as described in Fig. 4.

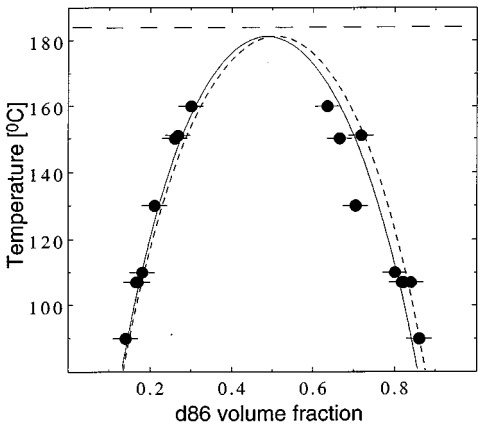

FIG. 8. Binodal for the blend $d86/h75$. From the binodal, the critical temperature for this blend is $T_c=181\pm4$ °C. Curves and broken horizontal line as described in Figs. 4 and 5.

fits based on the Flory–Huggins model, and will be discussed in detail in the next section. From such fits a value for T_c for each mixture is extracted. The critical temperatures derived from the coexistence curves 4–9 are denoted in bold type in Table II.

In order to estimate critical temperatures in other mixtures (for which the full coexistence curve was not determined) we adopted a simplified approach. In this we measured the NRA concentration-depth profiles for these mixtures at a smaller number of different temperatures, and without using an overlay layer to determine the absolute concentrations. This enables an accurate measure of the ratio $\alpha(T)\equiv\phi_2/\phi_1$ of the coexisting plateaus at each temperature T, as indicated in Fig. 3(a). The critical temperature T_c is then estimated by extrapolating to $\alpha(T)=1$, i.e., the temperature of complete interdiffusion. In practice we use the Flory–Huggins (FH) model[22,23] to optimize the extrapolation (caption to Fig. 10). The experimentally determined values of α are rather well described using this approach, as shown in Fig. 10 for several samples. Figure 10(d) demonstrates that

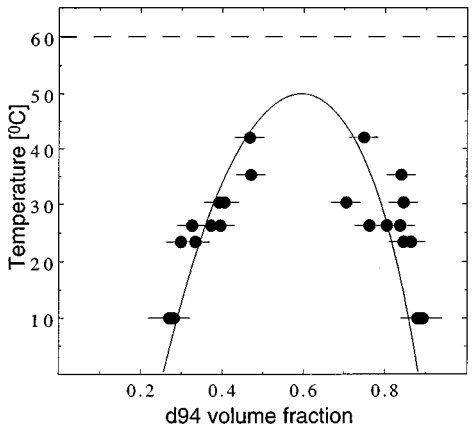

FIG. 9. Binodal for the blend $d94/h86$. From the binodal, the critical temperature for this blend is $T_c=50\pm6$ °C. The solid curve is the binodal calculated from the FH model with $\chi(T)=A/T$. Value of A given in Table III. The broken horizontal line as in Fig. 5.

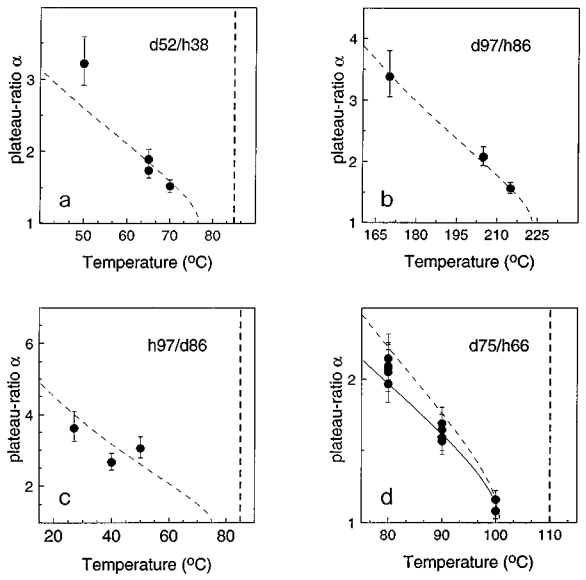

FIG. 10. Variation of the ratio of plateau compositions $\alpha(T)=\phi_2/\phi_1$ with temperature T for different blends as labeled in the figures, illustrating how T_c is extracted from such data. The vertical broken lines are temperatures at which full interdiffusion was observed, i.e., $T>T_c$. The broken curves are calculated from the FH model with $\chi(T)=A/T$, with A adjusted to provide the best fit to the data. The critical temperature is at the point of full interdiffusion, $\alpha(T=T_c)=1$. The values of A and T_c are given in Table III. Figure 10(d) shows data from the blend $d75/h66$ for which the full binodal was measured (Fig. 6). The solid line in 10(d) is calculated from the FH model with a composition dependent $\chi(T,\phi)=(A'/T+B)(1+v\phi)$ (parameters in Table III), demonstrating that in the vicinity of T_c the procedure is not sensitive to using a composition-dependent χ.

using FH with an interaction parameter having the simple form $X=(A/T)$ serves very adequately for this extrapolation. The accuracy of this procedure improves if the set of points is located close to T_c. Temperatures at which complete interdiffusion was observed are indicated by vertical broken lines in Fig. 10, and set upper limits on the respective critical temperatures. The values of T_c derived with this procedure are shown in Table II in normal type. We estimate the uncertainty in the value of T_c obtained by extrapolations as in Fig. 3 to be better than ±10 °C. In three of the mixtures, as indicated in Table II the bilayers were found to interdiffuse fully already at 30 °C (i.e., $T_c<30$ °C).

The final set of mixtures examined are those that showed little sign of mixing in the temperature range used. The criterion was set by the ratio of plateau compositions α: for bilayers where $\alpha(T)>6$ for $T\geqslant170$ °C (indicating a critical temperature above 250 °C) the blend is labeled by a cross "X" in Table II. Blends which have an even higher difference in their branching ratios x are expected to have yet higher critical temperatures, and were not examined in the present study; these combinations are labeled with dots "..." in Table II.

IV. DISCUSSION

A primary aim of the present paper is the determination of the phase coexistence characteristics in a series of E_{1-x}/EE_x random copolymer mixtures at different x values,

in order to shed light on the surface segregation and wetting properties from such mixtures (see companion papers II and III). The coexistence curves are, however, of considerable interest in themselves, not least because enabling the two phases to come to equilibrium and measuring the coexisting compositions provides by far the most direct way of determining the binodals in such high molecular weight polymers. In this our approach differs qualitatively from the more widely used scattering or other methods for probing the thermodynamics of such mixtures.

We note immediately that all coexistence curves (Figs. 4–9) have the general shapes expected from the classic polymer mixing models,[22] as discussed in more detail below. We also note, both from the binodals and from the summary of T_c values in Table II, that wherever critical temperatures were measured for mixtures with identical x_1 and x_2 values but with the deuterium labeling exchanged, i.e., $h38/d52$ vs $d38/h52$, $h66/d52$ vs $d66/h52$, and so on, the mixture which has the deuterium label on the copolymer with the higher ethylethylene content (higher x value) has a significantly higher critical temperature. This has earlier been noted in a number of studies for analogous mixtures of E/EE random copolymers.[13–15,24] The origins of this effect—which is equivalent to having larger mean segmental interactions in the mixtures where the higher x copolymer is deuterated—have been discussed at length,[13,14,24] and will not be considered further here.

A. Binodals and segmental interaction parameters

A reasonable starting point[25] at the mean field level for discussing both the spatial and the composition characteristics of coexisting profiles such as in Fig. 3 is the generalized Flory–Huggins–de Gennes expression for the excess free energy $\Delta\mathscr{F}$ in the bulk for two semiinfinite polymer phases A and B separated by a planar interface (at $z=0$), per unit area of the interface

$$\Delta\mathscr{F}/kT=\int_{-\infty}^{\infty}dz\left\{\Delta F_M-\Delta\mu\phi+\frac{a^2}{36\phi(1-\phi)}(\nabla\phi)^2\right\}. \tag{4}$$

Here ΔF_M is the Flory–Huggins free energy of mixing, $\Delta\mu$ is the chemical potential difference, a is the size of a polymer segment, $\phi\equiv\phi(z)$ is the local volume fraction of component A and the gradient term is with respect to z.

The Flory–Huggins (FH) model[22,23] for the free energy of mixing ΔF_M of two homopolymers A and B of degrees of polymerization N_A, N_B gives

$$\Delta F_M/k_BT=(\phi/N_A)\ln\phi+[(1-\phi)/N_B]\ln\phi+\chi\phi(1-\phi), \tag{5}$$

where $\phi\equiv\phi_A$ as before is the volume fraction of polymer A and χ is a segment–segment interaction parameter (normalized per monomer volume). This formulation is based on an assumption of incompressibility and no volume change on mixing, so that $\phi_A=(1-\phi_B)$. The form of Eq. (5) also assumes that the monomeric volumes v_1 and v_2 of the two polymers are identical (although this last constraint may be readily relaxed). The first two terms on the right-hand side (RHS) result from the entropy of mixing of the chains, and in the original FH model the interaction parameter χ is purely enthalpic: χk_BT is a constant assumed independent of N and of ϕ, i.e., $\chi=A/T$. We recall that the FH model applies to homopolymers, while we use random copolymers. For our purposes, in line with earlier discussions, we assume that the microstructure of our chains may be coarse grained so that we are dealing with ''homopolymers'' of effective mean microstructure defined by the extent of ethyl branching n_b (or x) in our chains.

Given a relationship between χ and T, we may readily use Eq. (4) to evaluate the coexistence curve.[25,26] For coexistence in the two phase region the coexisting compositions ϕ_1 and ϕ_2 at any temperature are obtained by minimizing the RHS of Eq. (4) far from the interface, in a region where $\nabla\phi\to0$. We start with the original (and simplest) assumption $\chi=A/T$. From the FH model[22,23] we expect the critical interaction parameter to be given by

$$\chi_c\equiv\chi(T=T_c)=(N_A^{1/2}+N_B^{1/2})^2/(2N_AN_B). \tag{6}$$

Putting $\chi_c=A/T_c$, and knowing the degrees of polymerization (Table I), the values of the constant A may be obtained for all couples for which the critical temperature has been determined (Table II). Using these values of A we have plotted the calculated binodals indicated by broken curves in Figs. 4–9. The first thing to note is that even at this level of simplicity (i.e., $\chi=A/T$) the curves fit the coexistence data very reasonably. For three of the mixtures, $d52/h66$ (Fig. 4), $d86/h75$ (Fig. 8) and $d94/h86$ (Fig. 9) the fits are indeed almost within the scatter of the data, while for $d75/h86$ (Fig. 7), $d75/h66$ (Fig. 6) and $d66/h52$ (Fig. 5) there is some (small) discrepancy (most marked for $d66/h52$), in particular concerning the position of the critical composition ϕ_c. Values of A for all couples are given in Table III. For completeness, we also include in Table III the values of A and T_c for the couples $d78/h88$ and $d88/h78$ determined earlier.[15] We

TABLE III. Critical temperatures for the E/EE blends determined either from the binodals of Figs. 4–9 or from the (ϕ_1/ϕ_2) vs T extrapolations (see, e.g., Fig. 10 and text). When not stated, the uncertainties in the values of T_c are estimated at 4 °C. The values of A in the third column are derived from the relation $A=\chi_cT_c$, with χ_c given by Eq. (6). The values of $\chi(T,\phi)=(A'/T+B)(1+v\phi)$ provide the best fit to the binodals in Figs. 4–8 and are determined as described in the text.

Blend	T_c[°C]	A	Interaction parameter $\chi(T,\phi)$*
$d52/h38$	77±7	0.422	⋯
$h52/d38$	50±10	0.390	⋯
$d66/h52$	204	0.548	$(0.327/T+3.48.10^{-4}).(1+0.222.\phi)$
$h66/d52$	88	0.415	$(0.452/T-1.2.10^{-4}).(1+0.031.\phi)$
$d75/h66$	101	0.413	$(0.371/T-2.7.10^{-5}).(1+0.212.\phi)$
$h75/d66$	33±10	0.353	⋯
$d86/h75$	181	0.578	$(0.559/T+8.10^{-5}).(1-0.057.\phi)$
$h86/d75$	97	0.471	$(0.547/T-8.10^{-5}).(1-0.217.\phi)$
$d88/h78$	127	0.557	$(0.502/T-8.2.10^{-5}).(1+0.323.\phi)$
$h88/hd78$	62	0.467	$(0.454/T-9.10^{-7}).(1+0.064.\phi)$
$d94/h86$	50±6	0.647	$0.647/T$
$d97/h86$	223±8	0.637	⋯
$h97/d86$	75±10	0.453	⋯

note that the values of the critical temperatures derived from our binodals are very close to values obtained by scattering experiments in the cases where identical mixtures ($d66/h52$, $h66/d52$, and $h88/d78$) were used.[10,11,27,28]

The original FH model as formulated in Eq. (5), with $\chi=A/T$, captures the essential physics of polymer mixing, in particular for materials where the van der Waals interactions are dominant, as in the polyolefins studied here, and its predictions for the coexistence curves are quantitatively rather good. However, the predictions of Eq. (5) may deviate from experiment even in simple model systems such as those in the present study, noted especially in Figs. 5, 6, and 7 where the critical volume fractions and the width of the binodal (Fig. 5) differ noticeably from those predicted. Theoretically, there have been several extensions to the original FH model to provide more realistic frameworks;[29–36] many of these discuss the role of mixture composition and other effects (including finite compressibilities, the actual shape of the monomers, and local density fluctuations) on the effective interaction parameter. In this discussion we do not attempt a detailed comparison of our binodals with these theoretical modifications; but there is some interest in examining the effect of a compositional dependence in the interaction parameter χ on the fit to our experimental coexistence data. In addition, for subsequent discussion of surface segregation properties (in II and III) we shall require a form of χ that adequately describes the experimental binodals.

To do this we choose a linear composition dependence

$$\chi(T,\phi)=(A'/T+B)(1+v\,\phi). \tag{7}$$

This is the simplest nontrivial dependence,[37] and its relation to other work is considered elsewhere.[38] This form for χ is used in Eq. (5) and the values of the parameters A', B, and v are chosen to yield the calculated binodal which best fits the coexistence data in Figs. 4–9.[39] The final values must be optimized simultaneously to provide the best fit, and the resulting variations $\chi(T,\phi)$ are given in Table III.

Some comments are in order concerning the $\chi(T,\phi)$ expressions in Table III. For completeness, the fits using the composition-dependent interaction parameter were carried out on all experimentally determined binodals, including those of the $h66/d52$ and $d86/h75$ couples where the simple $\chi=A/T$ form provides a reasonable fit of the data.[37] We note that the magnitude of B is in all cases much smaller than A/T (over the relevant T range studied), as would be expected from interactions dominated by dispersive (van der Waals) enthalpic contributions.[40] We note in particular that the magnitude of χ evaluated at the typical temperatures of our study using the $\chi=A/T$ form (with A given by $\chi_c\cdot T_c$, as in Table III) is very close to its value using the full ϕ-dependent form for all cases where $\chi(T,\phi)$ was evaluated.

Finally, we note that where identical blends have been studied both in this work and small-angle neutron scattering by (SANS)[10,11,27,28]—namely the couples $d66/h52$, $h66/d52$, and $h88/d78$—direct comparison may be made between $\chi(T,\phi)$ as determined from our binodals and $\chi\mathrm{SANS}(T,\phi)$ deduced from the scattering at different blend compositions. We find a close agreement between the interaction parameters determined by the two methods, both in terms of absolute values and in particular in the composition dependence of χ in the midrange composition regime $0.2<\phi<0.8$. This comparison is explored in detail elsewhere.[38]

The variation of interactions in these mixtures with chemical mismatch between the components is a central issue and has been addressed in previous studies of interactions in model polyolefin systems[13,14,24] as well as in recent theoretical discussions.[33,35,36,41] Here we adopt a simplified approach. Consideration of the effect of the exchange of isotope labeling on the interaction parameters in the E/EE blends suggests that averaging the interaction parameters $\chi(hx_1/dx_2)$,$\chi(hx_2/dx_1)$ for the two respective mixtures approximately eliminates the effect of isotopic interactions.[13,14,24,42] That is,

$$[\chi(hx_1/dx_2)+\chi(hx_2/dx_1)]/2\approx\chi(hx_2/hx_1)\equiv\chi(x_2/x_1). \tag{8}$$

This relation assumes that the degrees of deuteration in the two cases are equal or closely similar, and that interactions between monomers induced by the chemical mismatch, which we call $\chi_{E/EE}[\equiv\chi(1/0)]$, are much larger than those induced by isotopic d/h interactions, $\chi_{d/h}$. In practice both of these are well obeyed, with values of $\chi_{E/EE}$ and $\chi_{d/h}$ being $O(10^{-2})$ and $O(10^{-4})$, respectively. We note also that in all mixtures where interactions are averaged in this way, the degrees of polymerization are similar for both components, and in the range $N=1750\pm250$. We now take the canonical form $\chi=A/T$ for the interaction parameters for all the E/EE mixtures studied, with the A values listed in Table III. This procedure is well supported by our earlier considerations following Eq. (5). Direct independent support for its validity is provided by averages of critical temperatures based on light scattering studies in similar mixtures.[43] We then have

$$\begin{aligned}\chi(x_2/x_1).T&=\tfrac{1}{2}[\chi(hx_1/dx_2)+\chi(hx_2/dx_1)].T\\&=\tfrac{1}{2}[A(hx_1/dx_2)+A(hx_2/dx_1)]\\&=\overline{A}(x_1/x_2).\end{aligned}$$

We note that for a given (x_1/x_2) pair $\overline{A}=\overline{T}_c\chi_c$, where $\overline{T}_c$ is the critical temperature averaged over the $(dx1/hx2)$ and $(hx1/dx2)$ pairs, and χ_c is given by Eq. (6).

According to random copolymer theory,[44] one expects

$$\chi(x_2/x_1)=\chi(1/0)\Delta x^2, \tag{9}$$

where $\Delta x=(x_1-x_2)$. The value of $\chi(x_2/x_1)/(\Delta x)^2$ should then be a constant. In practice, as seen in Fig. 11, this quantity increases monotonically with the mean composition $\bar{x}=(x_1+x_2)/2$, a relation noted in earlier SANS studies,[28] and also in a very recent theoretical analysis.[45] In Fig. 11 we also include experimental points based on $\overline{T}_c$ determinations from earlier work by Rhee and Crist[13] and by Krishnamoorti *et al.*[27] These data, shown as solid symbols in Fig. 11, are derived from direct $\overline{T}_c$ determinations (in common with our results), and they fit well with our present data. For completeness, we include in addition in Fig. 11 (as open symbols) the values for the interaction parameters evaluated from

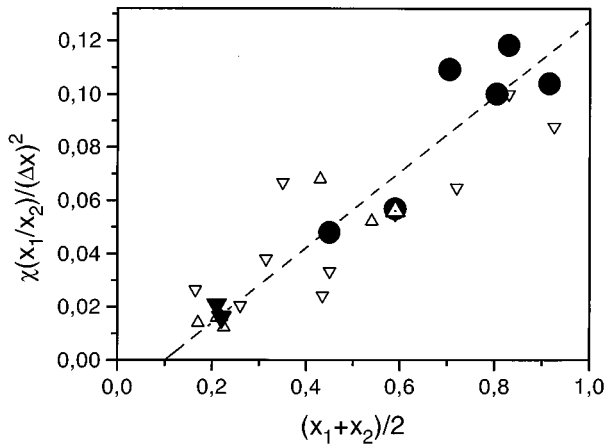

FIG. 11. The variation of $\chi(x_1,x_2)/\Delta x^2$, with $\bar{x}=(x_1+x_2)/2$, - ●, this study. $\chi(x_1,x_2)$ is given by $\bar{A}/T$, where $\bar{A}$ is the mean value of A for the blends dx_1/hx_2 and hx_1/dx_2 (Table III). Data based on $\bar{T}_c$ determinations are also given from Refs. 13 (▼) and 24 (△). Open symbols are for interaction parameters evaluated from SANS data from Refs. 13 (△) and 28 (▽). All data are adjusted to a reference temperature of 160 °C. Broken line—best fit to data.

scattering studies (Refs. 13 and 27). Within the scatter, the plot shows that $\chi(x_2/x_1)/(\Delta x)^2$ is reasonably correlated (linearly) with $\bar{x}$.

Finally we remark on the close linear correlation between χ and Δn_b (the difference in the extent of ethyl branching between the different components of the blend). The variation of χ with Δn_b is shown in Fig. 12 (at the same reference temperature 160 °C as in Fig. 11). Also shown in Fig. 12 are the data based on the earlier direct determinations of $\bar{T}_c$ for such E/EE mixtures[13,27] which also correlate well with Δn_b. The plot shows a clear monotonic variation, indicating a linear dependence $\chi \propto \Delta n_b$ over the range of the data. This dependence of the mean segmental interaction on the extent of chemical mismatch directly expressed in Δn_b is empirical, but is intuitively appealing. If we include the SANS-derived interaction parameters,[13,27] as is done in the inset to Fig. 12, χ continues to have a linear correlation with Δn_b, though the correlation becomes more scattered (the scatter is comparable with or somewhat smaller than that of Fig. 11).

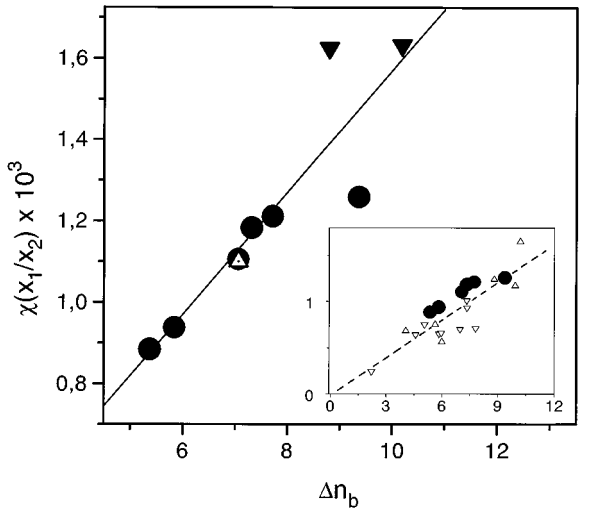

FIG. 12. The variation of $\chi(x_1,x_2)$ with the difference Δn_b in the number of ethyl branches (per 100 backbone units) between components x_1 and x_2, at a reference temperature 160 °C ● - this study. Data based on $\bar{T}_c$ determinations are also given from Refs. 13 (▼) and 24 (△). The inset shows the plot including $\bar{T}_c$-based $\chi(x_1,x_2)$ data from this study (●) and points evaluated from SANS data from Refs. 13 (△) and 28 (▽); broken line—guide to eye.

V. SUMMARY AND CONCLUSIONS

An understanding of the surface properties of polymer mixtures requires a knowledge of their bulk thermodynamics. We have used NRA composition versus depth profiling to determine miscibility, critical temperatures, and coexistence in model binary blends of E_{1-x}/EE_x random copolymers, one component of which is partly deuterated. Such depth profiling provides the most direct approach to determine binodals in polymer mixtures; we find that the shape of the binodals in well described using the simple Flory–Huggins formulation for the free energy of mixing, treating the copolymers as effective homopolymers with a mean segmental interaction parameter of the form $\chi=A/T$. (An even better fit can be obtained in some cases by allowing a weak composition dependence to be imposed on χ.) Extending earlier work, we find that the critical temperature in mixtures with a given value of (x_1,x_2) was in all cases higher when the deuterium label resided on the component with the higher ethyl branching fraction x.

Comparison with earlier SANS and light scattering studies on similar or identical E_{1-x}/EE_x mixtures showed good quantitative agreement between the results of the two methods. We conclude that determination of the binodals using NRA may provide a convenient and accurate alternative in many circumstances to the traditional scattering methods for determination of interactions in binary polymer mixtures. Within the range of our parameters, our results suggest that for such model polyolefin mixtures there is a reasonably good (linear) correlation between the magnitude of the interaction parameter χ and the extent of chemical mismatch, expressed as the difference Δn_b in extent of ethyl branching between the two components.

In the following papers (II and III) these data on the bulk interactions are used to discuss surface segregation behavior from these same model mixtures.

ACKNOWLEDGMENTS

We thank T. Kerle for very useful comments. Useful discussions with N. Balsara, K. Binder, W. W. Graessley, R. Krishnamoorti, and D. Lohse are acknowledged with thanks. We also thank the German-Israel Foundation (G.I.F.), the U.S.-Israel Binational Science Foundation (BSF), the Commission of the European Communities, the Minerva Foundation, and the Ministry of Sciences and Arts (Israel) for their support of this work.

[1] U. Steiner, J. Klein, E. Eiser, A. Budkowski, and L. J. Fetters, Science **258**, 1126 (1992).
[2] U. Steiner, J. Klein, and L. J. Fetters, Phys. Rev. Lett. **72**, 1498 (1994).
[3] U. Steiner, J. Klein, E. Eiser, A. Budkowski, and L. J. Fetters, Ber. Bunsenges. Phys. Chem. **98**, 366 (1994).
[4] U. Steiner, J. Klein, E. Eiser, A. Budkowski, and L. J. Fetters, in *Ordering in Macromolecular Systems*, edited by A. Teramoto (Springer, Berlin, 1994), pp. 313–329.
[5] R. L. Arnett and C. P. Thomas, J. Phys. Chem. **84**, 649 (1980).
[6] J. M. Carella, W. W. Graessley, and L. J. Fetters, Macromolecules **17**, 2775 (1984).
[7] A. Losch, R. Salamonovic, U. Steiner, J. Klein, and L. J. Fetters, J. Polym. Sci., Part B **33**, 1821 (1995).
[8] P. Hattam, S. Gauntlett, J. W. Mays, N. Hadjichristidis, R. N. Young, and L. J. Fetters, Macromolecules **24**, 6199 (1991).
[9] A. Zirkel, D. Richter, W. Pyckhout-Hintzen, and L. J. Fetters, Macromolecules **25**, 954 (1992).
[10] N. P. Balsara, L. J. Fetters, N. Hadjichristidis, D. J. Lohse, C. C. Han, W. W. Graessley, and R. Krishnamoorti, Macromolecules **25**, 6137 (1992).
[11] R. Krishnamoorti, W. W. Graessley, N. P. Balsara, and D. J. Lohse, Macromolecules **27**, 3073 (1994).
[12] J. C. Nicholson, T. M. Finerman, and B. Crist, Polymer **31**, 2287 (1990).
[13] J. Rhee and B. Crist, J. Chem. Phys. **98**, 4174 (1993).
[14] A. Budkowski, J. Klein, E. Eiser, U. Steiner, and L. J. Fetters, Macromolecules **26**, 3858 (1993).
[15] E. Eiser, A. Budkowski, U. Steiner, J. Klein, L. J. Fetters, and R. Krishnamoorti, ACS PMSE Proceedings **69**, 176 (1993).
[16] A. Budkowski, U. Steiner, J. Klein, and G. Schatz, Europhys. Lett. **18**, 705 (1992).
[17] U. K. Chaturvedi, U. Steiner, O. Zak, G. Krausch, and J. Klein, Phys. Rev. Lett. **63**, 616 (1989).
[18] U. K. Chaturvedi, U. Steiner, O. Zak, G. Krausch, G. Schatz, and J. Klein, Appl. Phys. Lett. **56**, 1228 (1990).
[19] J. Klein, Science **250**, 640 (1990).
[20] A. Budkowski, U. Steiner, and J. Klein, J. Chem. Phys. **97**, 5229 (1992).
[21] T. Flebbe, D. Burkhard, and K. Binder (unpublished).
[22] P. Flory, *Principles of Polymer Chemistry* (Cornell University Press, Ithaca, NY, 1971).
[23] P. G. de Gennes, *Scaling Concepts in Polymer Physics* (Cornell University Press, London, 1979).
[24] W. W. Graessley, R. Krishnamoorti, N. P. Balsara, L. J. Fetters, D. J. Lohse, D. N. Schulz, and J. A. Sissano, Macromolecules **26**, 1137 (1993).
[25] K. Binder, Acta Polymer. **46**, 204 (1995).
[26] K. Binder, J. Chem. Phys. 6387 (1983).
[27] R. Krishnamoorti, W. W. Graessley, N. P. Balsara, and D. J. Lohse, J. Chem. Phys. **100**, 3894 (1994).
[28] W. W. Graessley, R. Krishnamoorti, N. P. Balsara, R. J. Butera, L. J. Fetters, D. J. Lohse, D. N. Schulz, and J. A. Sissano, Macromolecules **27**, 3896 (1994).
[29] See R. Koningsveld, L. A. Kleintjens, and E. Nies, Croat. Chem. Acta **60**, 53 (1987) for a review to about 1986.
[30] M. Muthukumar, J. Chem. Phys. **85**, 4722 (1986).
[31] K. F. Freed, and A. I. Pesci, J. Chem. Phys. **87**, 7342 (1987); J. Dudowicz, K. F. Freed, and M. Lifschitz, Macromolecules **27**, 5387 (1994); K. F. Freed, J. Chem. Phys. (in press).
[32] K. Binder, Colloid Polym. Sci. **266**, 871 (1988).
[33] F. S. Bates, M. F. Schulz, and J. H. Rosendale, Macromolecules **25**, 5547 (1992).
[34] S. N. Kumar, Macromolecules **27**, 260 (1994).
[35] K. S. Schweitzer, Macromolecules **26**, 6050 (1993).
[36] A. J. Liu and G. H. Fredrickson, Macromolecules **27**, 2503 (1994); F. S. Bates and G. H. Fredrickson, Macromolecules **27**, 1065 (1994).
[37] We note that using a simple 1-parameter *parabolic* composition dependence of the form $\chi \propto [1+w\phi(1-\phi)]$ can only shift the critical composition towards 0.5, and such a dependence can therefore not improve the fits to the experimentally determined binodals, for example, in Figs. 5, 6, and 7.
[38] In preparation (1996).
[39] With the exception of the $d94/h86$ mixture where the scatter in the data was larger and where, in addition, the binodal was in reasonable agreement with a $\chi=A/T$ form.
[40] The very small value of B in some of the $\chi(T,\phi)$ expressions makes little discernible difference to the fit with the binodal, but for consistency we retain it as it derives from the optimization procedure.
[41] K. Freed and J. Dudowicz, Macromolecules (submitted).
[42] For example, in Ref. 14 the interaction parameter is evaluated as $\chi(hx_1/dx_2)=(x_1-x_2)^2\cdot\chi_{E/EE}+f_d^2\chi_{h/d}+2(x_1-x_2)f_d(\chi_{E/EE}\cdot\chi_{h/d})^{1/2}$, where f_d is the degree of deuteration of the deuterium-labeled component, $\chi_{E/EE}$ is the interaction due to the chemical mismatch and $\chi_{h/d}$ results from the isotopic interaction. For $\chi_{h/d}\ll\chi_{E/EE}$, and for f_d approximately equal on exchange of the label—both of which hold well in our mixtures—Eq. (8) follows immediately.
[43] Using the form $\chi=A/T$ together with Eq. (8), implies that for a given pair of copolymers specified by $\{x_i, x_j\}$ the following relations should hold for the critical temperatures: $T_c(hx_i/dx_j)+T_c(dx_i/hx_j)/2=T_c(hx_i/hx_j)=T_c(dx_i/dx_j)=\overline{T}_c$. This relation was checked explicitly, where T_c was determined by light scattering for all combinations of the pairs {0.35, 0.07}, {0.38, 0.06} by Rhee and Crist (Ref. 13) and the pair {0.66, 0.52} by Graessley *et al*. (Ref. 24), and shown to hold well.
[44] R. P. Kambour, J. T. Bendler, and R. C. Bopp, Macromolecules **16**, 753 (1983); G. Brinke, F. E. Karasz, and W. J. MacKnight, Macromolecules **16**, 1827 (1983).
[45] G. H. Fredrickson and A. J. Liu, J. Polym. Sci., Part B **33**, 1203 (1995).